Proceedings of the ASME 2010 3rd Joint US-European Fluids Engineering Summer Meeting and 8th International Conference on Nanochannels, Microchannels, and Minichannels
FEDSM-ICNMM2010
August 1-5, 2010, Montreal, Canada

FEDSM-ICNMM2010-30358

GENERAL MODELS FOR LINEAR DAMPING

HGD Goyder
Cranfield University
Shrivenham United Kingdom

ABSTRACT

The standard model for damping is the linear viscous dashpot which produces a force proportional to velocity. Although other sources of linear damping are known to exist, such as that due to viscoelasticity, it is not clear what range of mathematical forms damping models can take. Here it is suggested that there are only three types of damping model. These models are deduced by examining three configurations of mechanical components. These configurations include combinations of springs and dashpots and, most significantly, a semi-infinite beam. It is found that these models are best examined in the Laplace or *s*-plane so that features of the damping models may be expressed in terms of complex variable theory. The three types of damping model revealed by this analysis correspond to poles lying off the imaginary axis, poles on the negative real axis and pole like forms on the negative real axis that give rise to branch cuts. It is conjectured that these are the complete set of mathematical models that describe damping.

1 INTRODUCTION

What is the most general mathematical model for a mass-spring oscillator with arbitrary damping? When is the standard damping model of a linear viscous dashpot, in which the damping force is proportional to the velocity, adequate? How does damping influence a system with many degrees-of-freedom? How can damping be appropriately modeled in a computer simulation? It is surprising that all these questions remain open and that so little is known about damping and the way it influences structures.

This paper considers various alternative models for damping with the objective of understanding what mathematical form a general damping model may take.

Although numerical values for damping must be obtained from experimental measurements an experimental approach is not particularly fruitful in deducing the mathematical form of a damping model. This is because the inevitable errors associated with measurement mask underlying trends. Furthermore, it is not possible to fit damping data to a model unless there is a mathematical formulation for the model. Consequently, trying to examine damping experiments in the hope of seeing a damping model is problematic.

The approach taken here is to investigate combinations of components which exhibit damping and have a full mathematical description. In particular variants of mass-spring-dashpot combinations are examined. An important additional component, which is combined with a mass and springs, is the semi-infinite beam. This component does not depend on frequency in a simple way and is thus representative of a viscoelastic material.

In investigating the mathematical models for the effect of damping extensive use is made of complex variable theory. Thus the mathematical models are represented in the complex plane as complex frequency response functions. Although the complex frequency plane, in which complex values of the frequency ω (in radians per second), could be used it emerges that it is much simpler to use the complex *s*-plane in which $s = i\,\omega$ and $i = \sqrt{-1}$. The *s*-plane is the plane obtained when using the Laplace transform although it is often simpler to start in the frequency plane and then to convert to the *s*-plane.

The novel content of this paper is the identification of three types of damping which it is conjectured cover all possible damping forms.

The literature on damping is small with four text books providing most of the current thinking: Lazan[1], Nashif et al. [2], Mead [3] and Jones [4]. An early attempt at modeling damping was the hysteretic approach. This was well developed by Snowdon [5] but fails because it yields non-physical results. Another approach to damping has been developed by

Woodhouse [6] and by Woodhouse and Adhikari [7]. Their approach is a top down investigation which starts with multi-degree of freedom systems. Here a bottom-up approach is made which starts with a single-degree-of-freedom system.

2 NOMENCLATURE

A	Coefficient in partial fraction expansion of receptance
B	Coefficient in partial fraction expansion of receptance
C	Coefficient in partial fraction expansion of receptance
EI	Beam bending stiffness
M	Mass in beam system
R	Receptance = complex displacement / complex force
c	Dashpot coefficient
k	Spring stiffness
m	Mass or mass per unit length
s	Laplace variable
z	Complex variable
Ω	Non-dimensional frequency
α	Dimensionless stiffness ratio
β	Dimensionless damping ratio
ζ	Damping ratio
μ	Dimensionless beam factor
μ_0	Beam parameter
ω	Frequency in radians per second
ω_0	Dimensionless frequency

3 EXAMPLES OF DAMPING BEHAVIOUR

Some of the most interesting damping behaviour may be found by examining a viscoelastic material; Figure 1 shows a typical example. This data is tabulated in reference [4] and corresponds to a proprietary compound called LD-400. The data has been reworked from its original form and expressed as a receptance i.e. the ratio of the harmonic displacement due to an applied harmonic force and includes modulus and phase. The receptance has been normalised so that at zero frequency it has value 1.0. The huge dynamic range of the material should be noted with the frequency range covering 18 decades and the receptance a factor of 50. The empirical fit has also come from [4] and is given by the equation

$$R(\omega) = \frac{1 + (0.374155 + 0.0340455\,i)\omega^{0.47}}{1 + (2.29099 + 2.08464\,i)\omega^{0.47}} \qquad (1)$$

where R indicates the receptance and ω is the frequency in radians per second. Note that the frequency is raised to the power of 0.47. This is a fractional power and is the gradient of the sloping part of the modulus function. Viscoelastic materials exhibit a wide range of gradients that lie between 1 and 0. Although a good fit to the data the empirical formula is not satisfactory because for some frequency ranges it creates non physical features in the receptance. It is for this reason that physical components with exact receptance values are used within this investigation.

A spring-dashpot system that has been used in an attempt to model this material is given in Figure 2. Note that although this spring-dashpot system fits some of the data the gradient is too steep with a value of -1. The phase is also a very poor fit.

The measured data of Figure 1 shows the type of damping system for which mathematical models are required.

4 THE MASS-SPRING-DASHPOT-MODEL

The standard and simplest model for a damped oscillating system is shown in Figure 3. This system will be briefly reviewed as a template for other systems and to identify the first way in which damping enters a mathematical model.

The well known equation for the frequency response function of this system is

$$\frac{X}{F} = R(\omega) = \frac{1}{k + i\omega c - m\omega^2} \qquad (2)$$

where R is again the receptance and the symbols correspond to the labelled items in Figure 3. The equation may be reworked to throw most terms into a non-dimensional form as follows

$$R(\omega) = \frac{1}{k}\frac{1}{1 + 2i\zeta\dfrac{\omega}{\omega_0} - \dfrac{\omega^2}{\omega_0^2}} = \frac{1}{k}\frac{1}{1 + 2i\zeta\,\Omega - \Omega^2} \qquad (3a)$$

where

$$\omega_0 = \sqrt{\frac{k}{m}},\quad \zeta = \frac{c}{2m\omega_0},\quad \Omega = \frac{\omega}{\omega_0} \qquad (3b)$$

It is not possible to make all the terms non-dimensional and the stiffness k has been left un-normalised. This stiffness then becomes a reference value that is used in Equation 3b to make the other terms non-dimensional. Equation 3a may also be expressed in the Laplace s-plane by writing

$$R(s) = \frac{1}{k}\frac{1}{1 + 2\zeta s + s^2} \qquad (4)$$

where the correspondence with the frequency response function is made by setting $s = i\,\Omega$.

The denominator is a quadratic function in s with real coefficients. The fundamental theorem of algebra states that the denominator has either two real roots or two complex conjugate roots. For $\zeta < 1$ the two roots are complex while for $\zeta > 1$ the two roots are real. If $\zeta = 0$ there is no damping and the roots are pure imaginary and equal to $\pm\, i$. Figure 4 shows these possibilities for the location of the roots on the complex plane. The roots of the denominator correspond to poles of the receptance function.

This is the first mathematical model for damping. The damping, when modelled in the complex *s*-plane, causes a shift of the poles of the un-damped system which takes them off the imaginary axis into the left half plane. With large damping the poles are shifted onto the negative real axis.

5 VARIANTS ON MASS-SPRING AND DASHPOT MODELS

Figure 5 (*a*) and (*b*) show a mass with two springs and a dashpot. This configuration captures some of the attributes of the viscoelastic material described in section 3. At low frequencies the dashpot produces only a small force and stiffness dominates. Alternatively, at high frequencies the dashpot produces a large force and may lock-up (i.e. have little motion), again stiffness will dominate. Thus there is a frequency range within which the damper can operate. The two configurations in Figures 5 (*a*) and (*b*) lead to very similar equations for the frequency response function and consequently just configuration 5 (*a*) will be developed.

The receptance for the system in Figure 5 (a) is

$$\frac{X}{F} = R(\omega) = \\ = \frac{-c\omega + i k_2}{c m\omega^3 - i k_2 m\omega^2 - c\omega(k_1 + k_2) + i k_1 k_2} \tag{5}$$

A non-dimensional form may be developed by defining dimensionless parameters α, β and Ω as follows.

$$\frac{k_2}{k_1} = \alpha, \quad \frac{c}{2\sqrt{m k_1}} = \beta, \quad \frac{\omega}{\sqrt{\frac{k_1}{m}}} = \Omega \tag{6}$$

These parameters represent the ratio of the two stiffnesses, a normalised dashpot coefficient and a non-dimensional frequency. In terms of these parameters and converting to the *s*-plane the receptance becomes

$$R(s) = \frac{1}{k_1}\frac{2\beta s + \alpha}{2\beta s^3 + \alpha s^2 + 2\beta s(1+\alpha) + \alpha} \tag{7}$$

The denominator of the receptance is a cubic in *s* and thus may be expanded by means of a partial fraction decomposition. Two forms are possible depending on whether the denominator has three real roots or one real root and a pair of conjugate complex roots. (These two possibilities are proscribed by the fundamental theorem of algebra.)

The case with three real roots may be written

$$R(s) = \frac{1}{k}\left[\frac{A_1}{s - r_1} + \frac{A_2}{s - r_2} + \frac{A_3}{s - r_3}\right] \tag{8}$$

where r_1, r_2 and r_3 are the three roots (all on the negative real axis of the *s*-plane) and A_1, A_2 and A_3 are the residues of the poles (all real values).

The case with one real root and a pair of complex conjugate roots may be written

$$R(s) = \frac{1}{k}\left[\frac{A + sB}{s^2 + 2\zeta\,\Omega_0\, s + \Omega_0^2} + \frac{C}{s - r}\right] \tag{9}$$

where *r* is the real root and the conjugate complex roots have been combined to give the denominator of the standard single-degree of freedom model. This not only gives meaning to the receptance but makes all parameters including *A*, *B* and *C* real. This receptance can be viewed as a single-degree-of-freedom system to which an additional term has been added. All the parameters ζ, Ω_0, *r*, *A*, *B* and *C* depend on the normalised stiffness ratio α and normalised damping β .

Figure 6 (a) and (b) identify the behavior of Ω_0 and ζ as α and β are varied. The region in which there are three real roots is contained between the lines label *AOB* with *O* being located at the point α = 8 and $\beta = 4/\left(3\sqrt{3}\right) \approx 0.7698$. These lines are found by determining the discriminant of the denominator in Equation 7.

The region underneath *OB* is the case where the stiffness k_2 is large compared to k_1 and consequently the system looks like the standard single-degree-of-freedom system of Figure 3. However, above the line *OA* the system has a large dashpot and a large stiffness k_2. In this case the stiffness k_1 is negligible and as the dashpot value is increased it locks-up causing the natural frequency to increase and the damping ratio to decrease.

This configuration of a mass with two springs and a dashpot gives rise to the second damping model. Here as well as there being damping associated with poles lying off the imaginary axis there is at the same time a pole on the negative real axis. Generalizations of this damping model in which more poles are present on the negative real axis are considered in section 7.

6 BEAM DAMPERS

A beam of infinite length may carry waves to infinity with no reflected waves returning; it therefore represents a system which absorbs energy. The significant feature of an infinite beam is that it has a frequency response function that is a fractional power of frequency. In this way it is similar to a viscoelastic material. Thus when such a beam is incorporated into a damping system it gives an exact mathematical model that can be fully analysed. This avoids the difficulties of the non physical model found in the empirical fit of the viscoelastic material.

Figure 7 shows a configuration in which a mass on a spring is located near the intersection of two beams which are considered infinite. This is a plausible model for a machinery installation in a building.

Figure 8 shows a development of this system in which there is a spring, k_1 which represents the static stiffness of the system. The beam *AB* is considered to be a rigid lever of length *L* which inputs vibration into the infinite flexible beam *BC*.

The two springs in Figure 8 act like those in Figure 5 and control the low frequency and high frequency behaviour.

The receptance of the lever at point *A*, in the absence of the spring is given by

$$R(\omega)=\frac{L^2}{\sqrt{2}\left((E\,I)^3 m\right)^{\frac{1}{4}}\sqrt{i\,\omega}}=\frac{1}{\mu_0\sqrt{i\,\omega}} \tag{10}$$

where $E\ I$ is the bending stiffness of the beam (modulus of elasticity times second moment of area about the neutral plane) and m is the mass per unit length of the beam. Note the fractional power (square root) of frequency in this receptance. In the second form of the equation the mechanical properties have been consolidated into a parameter μ_0.

The square root of frequency in the receptance requires some special attention because it is multivalued and furthermore must take complex values. In complex variable theory such functions require the definition of a branch cut so that just one of the complex values may be considered at a time. The selection of the branch cut will be delayed until the final receptance and its conversion to the *s*-plane has been established.

The receptance of the whole system in Figure 8, due to the force applied to the mass, may be constructed by combing the mass and the two springs with the receptance of the infinite beam to give the following expression

$$\begin{aligned}\frac{X}{F}&=R(\omega)=\\&=\frac{k_2+\mu_0\sqrt{i\,\omega}}{k_1k_2+\left(k_1+k_2-\omega^2M\right)\mu_0\sqrt{i\,\omega}-\omega^2M\,k_2}\end{aligned} \tag{11}$$

This receptance may be thrown into a non-dimensional form along the same lines as that used in Section 3 and Section 4. The non-dimensional form in the frequency and *s*-plane are given by

$$\begin{aligned}R(\Omega)&=\frac{1}{k_1}\frac{1}{1+\alpha-\Omega^2-\dfrac{\alpha^2}{\alpha+\mu\sqrt{i\,\Omega}}}\\R(s)&=\frac{1}{k_1}\frac{\alpha+\mu\sqrt{s}}{\alpha+(1+\alpha)\mu\sqrt{s}+\alpha\,s^2+\mu\,s^2\sqrt{s}}\end{aligned} \tag{12}$$

where the following substitutions have been made

$$\alpha=\frac{k_2}{k_1},\quad \mu=\mu_0\frac{1}{k_1}\left(\frac{k_1}{M}\right)^{\frac{1}{4}},\ \ \Omega=\frac{\omega}{\sqrt{\dfrac{k_1}{M}}},\quad s=i\,\Omega \tag{13}$$

The presence of the $\sqrt{s}$ on the denominator and numerator means that Equation 12 cannot be expressed in terms of a partial fraction expansion. Consequently some further manipulation is required in order to gain some understanding. Figure 9 shows the complex *s*-plane that will be used to describe the features of Equation12. The wiggly line drawn from $-\infty$ to 0 is a branch cut which is introduced to select one value of the square-root function. All values of *s* are restricted to have an argument, θ, that is limited to $-\pi<\theta\le\pi$. Numerical evaluation indicates that there is a pair of complex poles in the left hand side of the complex s-plane; these are also shown. These poles exist for all positive values of α and μ.. The existence of these poles has been established numerically. No case has been found where the poles are located on the real axis. A mathematical proof of their existence within the left plane with the exclusion of the real axis has yet to be found.

The form of Equation 12 and Figure 9 gives the third form of damping model. Here as well as poles off the imaginary axis there are branch-cut features that contribute to the damping.

In order to further understand the branch-cut features and to simplify Equation 12 the following substitution is made to remove the square root

$$\sqrt{s}\Leftrightarrow z\ \text{ or }\ s\Leftrightarrow z^2 \tag{14}$$

It should be noted that the transformation is not fully reversible since there are values of *z* that cannot be reached by the square root of *s* according to the branch-cut restriction of Figure 9. The result of making the transformation from *s* to *z* is to turn Equation 12 into a simple ratio of two polynomials given by

$$R(z)=\frac{\alpha+\mu\,z}{\alpha+\mu\,(1+\alpha)z+\alpha\,z^4+\mu\,z^5} \tag{15}$$

The denominator of Equation 15 is a polynomial of order 5 and has real coefficients. There are thus three possibilities for roots: 5 real roots or 3 real roots and one complex conjugate pair or one real root and 2 pairs of complex conjugate roots.

The results of a numerical investigation are shown in Figure 10. The lines *OA* and *OB* are found by determining the discriminant of the denominator of Equation 15. As the parameter space of α and μ is divided into just two regions only two of the above possibilities occur for roots. It is found that the case of one complex pair occurs within *OAB* and that outside this region there are two complex pairs.

These two regions give rise to two possibilities for the partial fraction decomposition. The general form of the partial fraction decomposition of Equation 15 is

$$R(z)=\frac{A_1}{z-z_1}+\frac{A_2}{z-z_2}+\frac{A_3}{z-z_3}+\frac{A_4}{z-z_4}+\frac{A_5}{z-z_5} \qquad (16)$$

where the z_i are the five roots of the denominator and the A_i are the residues of each pole. At least two of the roots will be complex conjugate pairs and if the values of α and μ lie outside *AOB* then there will be two such pairs. The values of the roots and of the residues all depend on the values of α and μ.

Following the partial fraction decomposition on the *z*-plane it is necessary to invert the transformation to find an expression in the *s*-plane. To facilitate this transformation let the first two terms of Equation 16 correspond to the complex pair that will remain in the *s*-plane. (The other roots will not be found on the *s*-plane but will express themselves through the branch-cut.). Now add the additional terms

$$-\frac{A_1}{z+z_1}+\frac{A_1}{z+z_1}-\frac{A_2}{z+z_2}+\frac{A_2}{z+z_2} \qquad (17)$$

which deliberately sum to zero adding nothing. The modified version of Equation 16 can now be written

$$\begin{aligned} R(z)=&\frac{2A_1z_1}{z^2-z_1^2}+\frac{2A_2z_2}{z^2-z_2^2}+ \\ &+\frac{A_1}{z+z_1}+\frac{A_2}{z+z_2}+\frac{A_3}{z-z_3}+\frac{A_4}{z-z_4}+\frac{A_5}{z-z_5} \end{aligned} \qquad (18)$$

where terms have been combined to give a quadratic form that is convenient for conversion back into the *s*-plane. Converting back into the *s*-plane using the transformation in Equation 14 gives

$$\begin{aligned} R(s)=&\frac{A+sB}{s^2+2\zeta\,\Omega_0\,s+\Omega_0^2}+ \\ &+\frac{A_1}{\sqrt{s}+z_1}+\frac{A_2}{\sqrt{s}+z_2}+\frac{A_3}{\sqrt{s}-z_3}+\frac{A_4}{\sqrt{s}-z_4}+\frac{A_5}{\sqrt{s}-z_5} \end{aligned} \qquad (19)$$

Here the first term corresponds to the standard form of a single-degree-of-freedom system with a damping ratio and natural frequency. The remaining terms do not have roots on the complex plane and because of their square root dependence are simple terms involving the branch cut.

This is the typical mathematical form for the third form of damping model.

7 GENERAL FORM FOR DAMPING

As a consequence of investigating the response of a mass-spring system with various examples of damping components three types of mathematical model for damping have been identified.

To summarise:

i) Damping associated with off-imaginary-axis poles.
ii) Damping associated with poles on the negative real axis.
iii) Damping associated with branch cut behaviour.

The first damping model is familiar from the standard study of the single-degree-of-freedom system. The other two types of damping give rise to terms which are additional to that of the single-degree-of-freedom model. These terms disappear as damping is set to zero.

These forms of damping can be easily generalised. For example, in Figure 11 the second form of damping is extended to have several poles by adding further springs and dashpots.

Similarly the beam damper can be generalised by considering a dependence on frequency that depends on other fractional powers. Mixtures of these models are also possible. However, whatever generalisations are used the resulting forms can be categorised as belonging to one of the three types listed above. It is conjectured that this applies to all damping models. Furthermore the simplification of the equations to that given above (by means of partial fractions or the generalisation of partial fractions for the third type) may prove to be useful.

8 DISCUSSION

The partial fraction expansion of the frequency response functions leads to a convenient mathematical form for further study. In particular, it would be nice to know when terms are important or can be ignored. This is not an easy task and may depend on the circumstances in which the model is used. If for example the model is part of a larger system and damping is important it is not clear how the damping of the whole system will depend on the details of the model.

A useful observation for those taking measurements and fitting mathematical models is that it is always correct to fit a single-degree-of-freedom system. Note that each of the models has this as one term. However, this work has shown that the single-degree-of-freedom model may not be sufficient and that more terms may be required.

The use of the *s*-plane has been particularly satisfactory. In this transformation the frequency response functions have all real coefficients. This simplifies numerical work and makes the identification of complex conjugate terms straightforward.

It is suggested that there can be no other forms of damping than the three types identified here. This suggestion is based on the idea that there are a limited number of features that the complex plane can exhibit while still maintaining, as it must, an analytic domain in the right half plane. It should be noted that except for the off-axis poles all the other features are associated with the negative real axis. This is perhaps necessary because features away from the axis would lead to oscillatory behaviour.

9 CONCLUSIONS

The following conclusions may be drawn.

1. The study of damped dynamic systems that are based on theoretical models rather than experimental data allows a deep and full understanding of general linear damping behaviour.
2. Mass-spring-damping systems may be conveniently analysed in the frequency domain and the Laplace s-plane. The s-plane is particularly convenient because coefficients of the frequency response function are real and complex conjugates may be easily identified.
3. The behaviour of an infinite beam provides an example of a damping mechanism that is frequency dependent (with frequency raised to a fractional power) in a manner similar to a viscoelastic material.
4. A method of breaking down a frequency response function into a number of terms which can be studied independently has been developed. For some cases this is just a partial fraction decomposition. However, a method for decomposing a rational polynomial involving fractional powers has also been developed and illustrated.
5. When expressed in a decomposed form the well known single-degree-of-freedom system is always present as one of the terms. However, the presence of damping creates additional terms that have been revealed by this analysis.
6. Damping emerges in mathematical models in three ways. Firstly it causes poles on the imaginary axis to move into the left hand side of the complex *s*-plane. Secondly, it results in poles on the negative real axis and thirdly it gives rise to branch-cut terms which can be written in pole-like forms.

ACKNOWLEDGMENTS

The author acknowledges the support of Cranfield University in the development of this research.

REFERENCES

[1] B J Lazan *Damping of Materials and Members in Structural Mechanics.* Oxford Pergamon Press 1968

[2] A D Nashif, D I G Jones and JP Henderson, *Vibration Damping*, John Wiley & Sons, 0-471-86772-11985

[3] DJ Mead, *Passive Vibration Control*, John Wiley and Sons, Chichester, UK 1998.

[4] DIG Jones, *Handbook of Viscoelastic Vibration Damping*, John Wiley and Sons Ltd, 2001.

[5] JC Snowdon. *Vibration and Shock in Damped Mechanical System.* Wiley, New York, 1968.

[6] J. Woodhouse, *Linear Damping Models For Structural Vibration*, Journal of Sound and Vibration, Volume 215, Issue 3, 20 August 1998, Pages 547-569.

[7] S. Adhikari, J. Woodhouse, *Identification Of Damping: Part 1, Viscous Damping*, Journal of Sound and Vibration, Volume 243, Issue 1, 24 May 2001, Pages 43-61

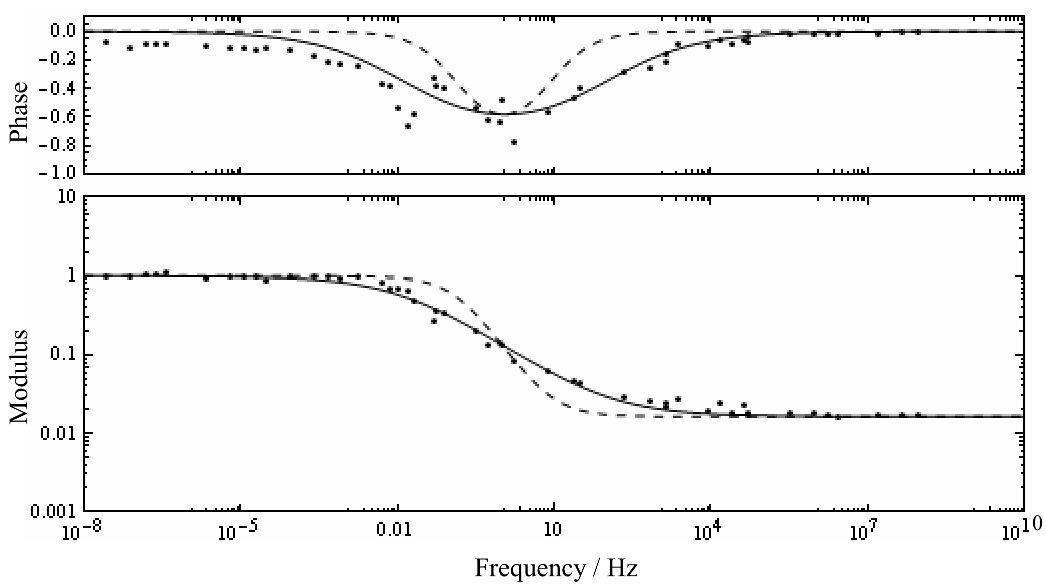

Figure1. A normalised modulus and phase for a viscoelastic receptance, • measured data, – empirical fit and - - - spring-dashpot model.

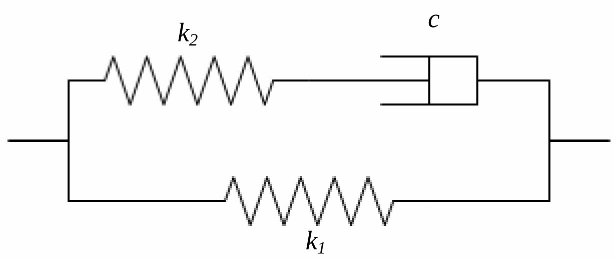

Figure 2. A two-spring-dashpot combination representing a damping system. Springs k_1 and k_2 with dashpot c.

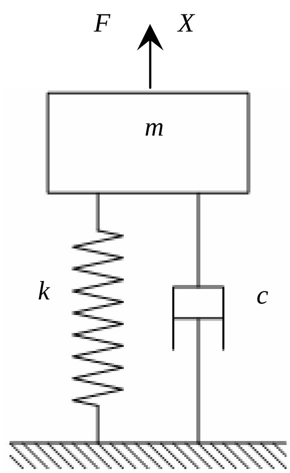

Figure 3. The standard mass-spring-dashpot system with stiffness k, dashpot coefficient c and mass m. The harmonic force amplitude and displacement response are F and X.

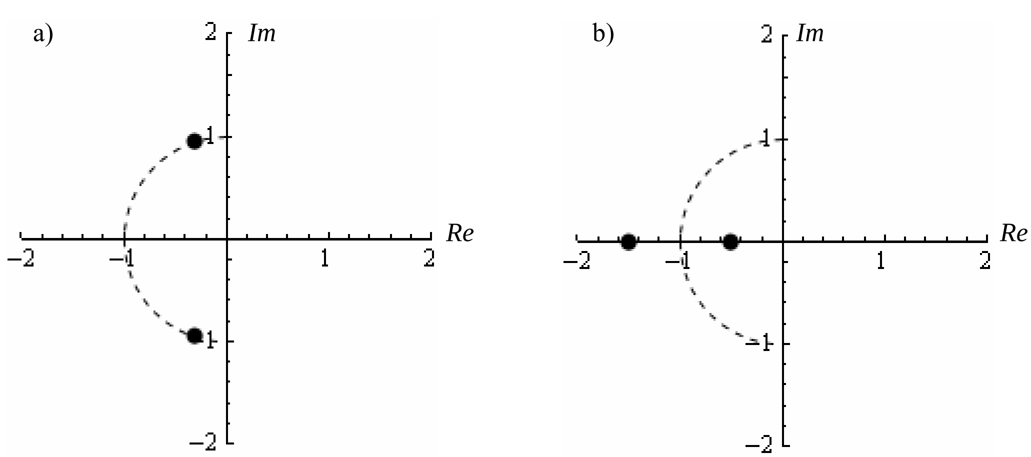

Figure 4. Location of poles of Equation 4 on the complex s-plane. a) $\zeta < 1$ and b) $\zeta > 1$

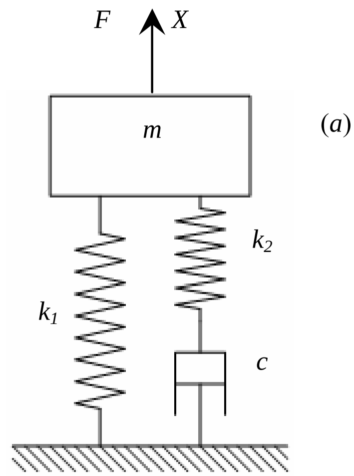

Figure 5. Two variants of a mass-two-spring-dashpot system. Springs k_1 and k_2 with dashpot c. The harmonic force amplitude and displacement amplitude are F and X.

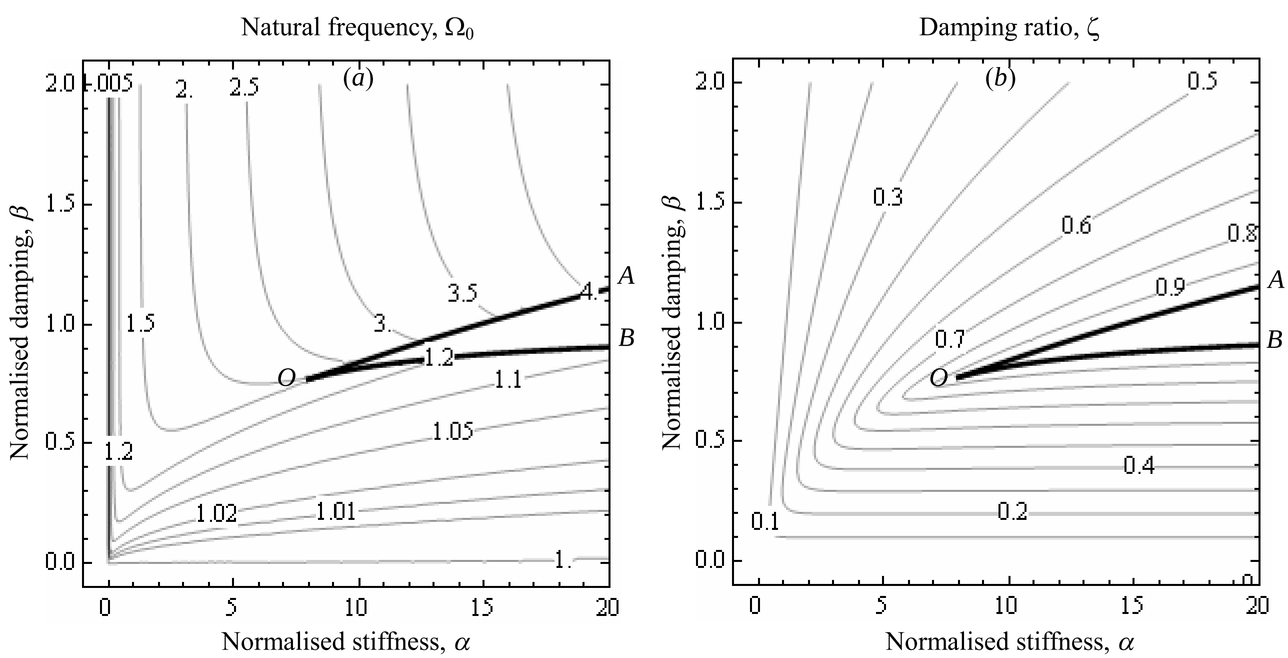

Figure 6. Behavior of (a) natural frequency and (b) damping ratio in quadratic denominator of Equation 9

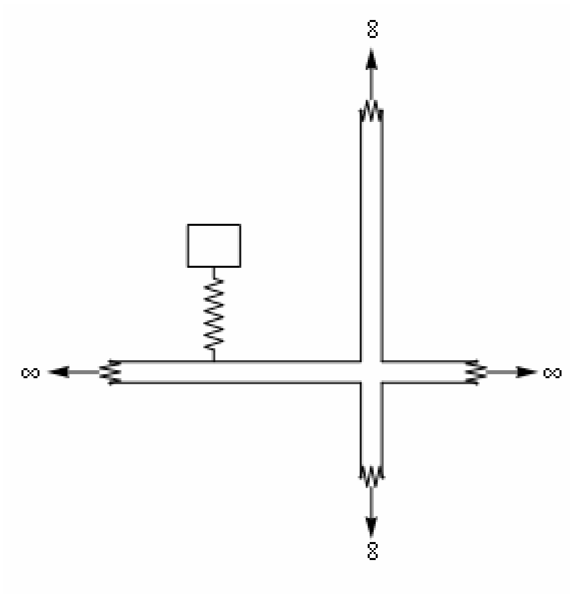

Figure 7. A mass-spring system connected to a system of infinite beams.

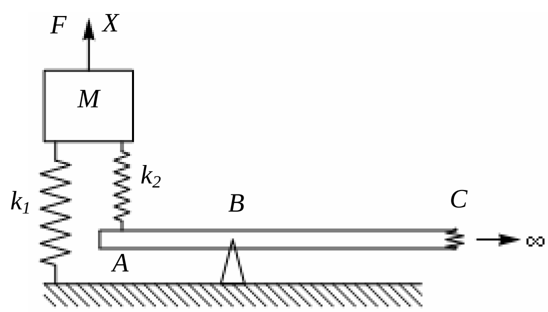

Figure 8. A mass on two springs is attached to a lever A B which operates an infinite flexible beam B C.

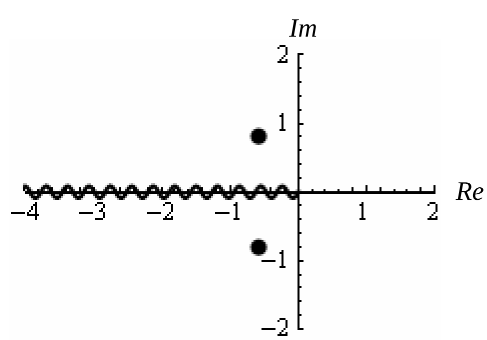

Figure 9. The complex *s* –plane showing the location of the branch cut (wiggly line) and the two poles of Equation 12

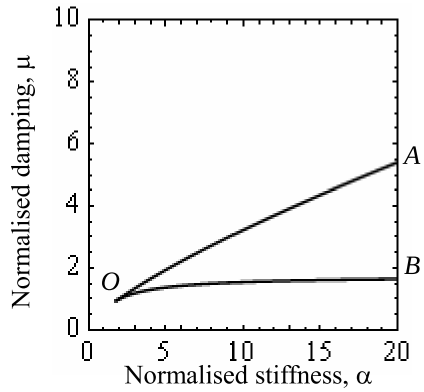

Figure 10. Regions of pole combinations for Equation 15. Within *AOB* one pair of conjugate roots, outside *AOB*, two pairs of conjugate roots.

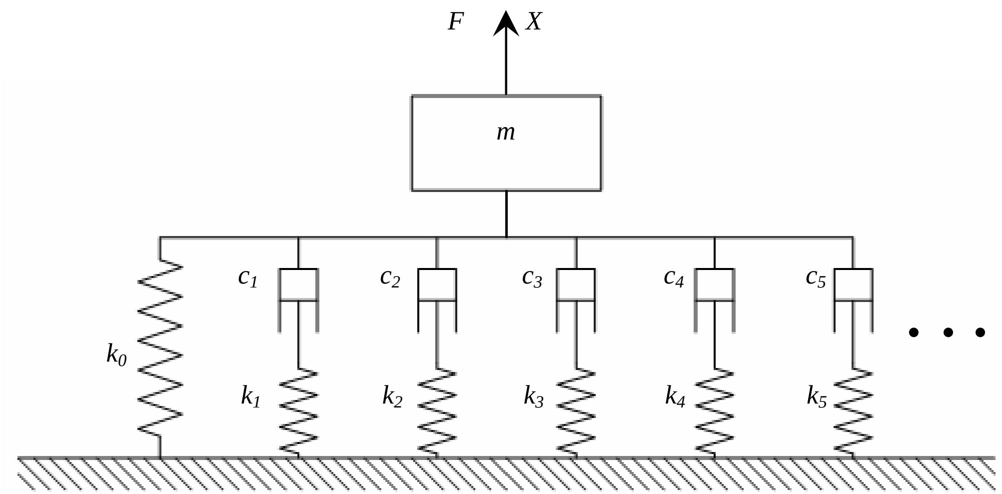

Figure 11. A generalisation of Figure 5 to many springs and dashpots. The dots indicate where additional items could be placed.